Progress In Electromagnetics Research C, Vol. 15, 75–87, 2010

A STACKED RING-PATCH ARTIFICIAL SUBSTRATE TO IMPROVE THE ANTENNA PERFORMANCE

M. N. Sujatha and K. J. Vinoy

Electrical Communication Engineering
Indian Institute of Science
Bangalore 560012, India

Abstract—In this paper, a stacked ring-patch two layer planar artificial substrate is analyzed numerically and is shown to possess the properties of a high impedance surfaces (HIS). Its properties are evaluated by investigating the surface wave propagation and plane wave reflection characteristics. Its application to reduce the mutual coupling of microstrip antennas and to improve the radiation pattern are investigated by simulation tool CST microwave studio. Experimental measurements using a pair of monopoles are used to confirm the surface waves suppression band. One of the main advantages of the proposed geometry is that it is simple and planar in nature, without the need for any via connections across dielectric layers and thus can be realized by planar technologies. Another advantage is that it exhibits over lapped surface wave suppression and in-phase reflection bands. Also it can be scalable to operate in different frequency range.

1. INTRODUCTION

In recent years there has been an increasing interest in artificial materials such as metamaterials, high impedance surfaces (HIS), artificial magnetic conductors (AMC), and electromagnetic band-gap (EBG) structures. Consisting of periodic structures such as metal patches printed on a metal-backed dielectric slab, many of these structures can be used for surface wave suppression and as a artificial magnetic conductor with zero phase shift [1]. The periodicity of these geometries are very much less than the operating wavelength.

Most of the structures used for suppressing TM surface waves have vias connected from top patches to the ground plane [1–4]. Their

Received 18 June 2010, Accepted 20 July 2010, Scheduled 2 August 2010
Corresponding author: M. N. Sujatha (mnsujathaguddu@rediffmail.com).

propagation characteristics are analyzed using a dispersion diagram. Although planar structures have been proposed recently as artificial magnetic conductors, their surface wave suppression characteristics are not demonstrated [5, 6]. In [7] planar structure is proposed for surface wave suppression, but the surface wave suppression band is at higher frequency for given dimension than via structures. One more factor observed in [7] is surface wave suppression. In phase reflection frequency bands are far from each other, and they are not overlapping. In this paper, we propose a planar configuration for high impedance surface and demonstrate the surface wave suppression and in-phase reflection characteristics. Since the proposed geometry is simple compared to the structure proposed in [7] and truly planar in nature without the need for any vias, it can be easily implemented using planar technology. The electromagnetic performance of this geometry is comparable to those proposed in recent literature using non-planar geometries [1–4].

2. STACKED RING-PATCH ARTIFICIAL SUBSTRATE

The geometry of the proposed stacked ring-patch two layer planar artificial substrate is shown in Fig. 1.

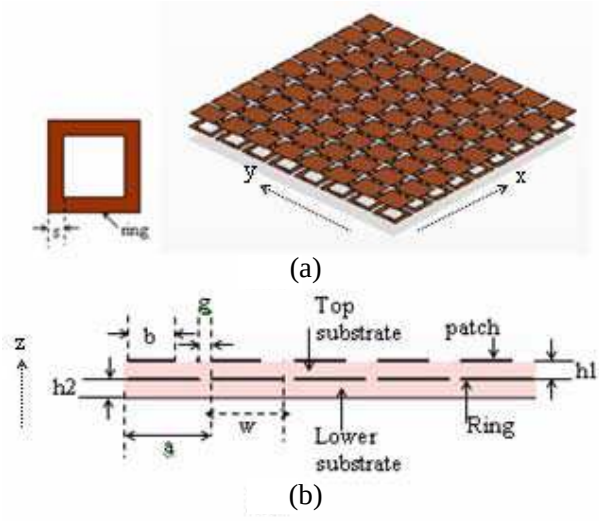

Figure 1. Geometry of the proposed stacked ring-patch two layer structure. (a) Array of the proposed structure. (b) Side view, $w + g = a$, $a = 3.5\,\text{mm}$, $w = 3\,\text{mm}$, $g = 0.5\,\text{mm}$, $s = 0.5\,\text{mm}$ $h_1 = h_2 = 0.787\,\text{mm}$, $b = 2.5\,\text{mm}$.

It is a periodic array of electrically small unit cells in x and y directions as shown in Fig. 1(a), whose side view is shown in Fig. 1(b). Metallic square rings of width 's' are printed on the metal backed lower substrate with a small gap 'g' between the rings. Metal square patches with width 'b' are printed on the top substrate. The arrays of metal patches and rings have the same periodicity 'a'. As long as the size and spacing of the elements are much smaller than the electromagnetic wavelength of interest, incident radiation cannot distinguish the collection of elements from a homogeneous material [8]. The arrays of metal patches and rings have the same periodicity 'a', yet these are offset as shown in Fig. 1(b). Offsetting of patches with respect to rings as shown in Fig. 2 increases the surface wave suppression level compared to the structure without offsetting. From the simulation results it is observed that offsetting should be such that patch must cover the ring 80% or greater. Offsetting of patch from ring does not affect the reflection properties of the structure. Ring width 's' affects the operating frequency of the structure. As the ring width reduces, suppression and reflection bands shift to lower frequencies.

3. SIMULATION STUDIES

Presently for the proposed structure analytical formulas are not fully developed to relate the structural parameters of the HIS to its

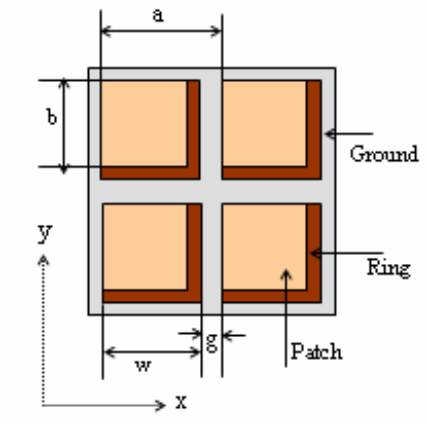

Figure 2. Four unit cells are enlarged to show dimensions $a = 3.5\,\text{mm}$, $w = 3\,\text{mm}$, $b = 2.5\,\text{mm}$, $g = 0.5\,\text{mm}$, $s = 0.5\,\text{mm}$.

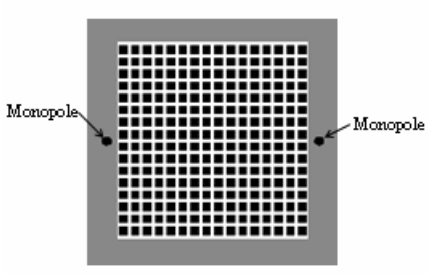

Figure 3. Simulation setup to find transmission (S_{21}) characteristics.

electromagnetic response. Usually the performance of the HIS is evaluated using fullwave electromagnetic numerical simulation software tools by direct and indirect approaches. The direct method consists of extracting the scattering parameters (S-parameters) between two ports placed across a planar array of the structure [1]. A second numerical procedure is indirect and involves extracting the dispersion diagram from an extensive procedure [1, 2]. The former approach is used in this study and discussed in the following paragraphs. In this study a two dimensional array of 16×16 unit cells, as shown in Fig. 3, is analyzed using simulation tool CST microwave studio.

3.1. Surface Wave Bandgap

As a measure of the TM_0 surface wave suppression band, the transmission across the structure is evaluated by introducing two radiators on either side of the array. Two monopoles of height 8 mm are used in this study, one for transmission and the other for reception. The geometrical parameters of the proposed structure under consideration are $w = 3$ mm, $a = 3.5$ mm, $g = 0.5$ mm, $s = 0.5$ mm, $b = 2.5$ mm and $h_1 = h_2 = 0.787$ mm. There are two layers in the structure, lower layer (mentioned in Fig. 1b as lower substrate) and top layer (mentioned in Fig. 1b as top substrate). Substrate Arlon AD600 of thickness 0.787 mm is used in both of the layers. Both the top and lower substrates have the same dimension equal to 60 mm $\times$ 60 mm. Dielectric constant of substrate Arlon AD600 is 6.15.

The transmission between monopoles shown in Fig. 4 proves the existence of a band-gap between 8 GHz and 9.6 GHz, in which the signal is strongly attenuated when the proposed geometry is placed between

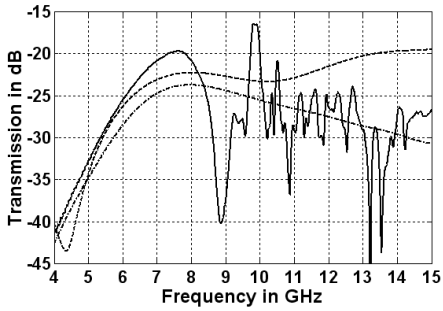

Figure 4. Transmission (S_{21}) between monopoles: ——— with proposed structure; - - - - - - with a grounded dielectric slab; - · - · - · with metal sheet only (no dielectrics).

the monopoles. For comparison propose the simulations were carried out to find the transmission between the two monopoles at the same distance on the same ground plane with metal sheet and dielectric slabs. Simulated transmission (S_{21}) plots are shown in Fig. 4. The increase in the transmission coefficient with the dielectric slab shows the presence of surface waves. These are suppressed within a band centered around 9 GHz.

3.2. Reflection Characteristics

In contrast to a perfect electric conductor, a magnetic conductor shows no phase shift on reflection. Reflection properties of the structure can be obtained by computing the phase of the reflection coefficient. HIS acts as artificial magnetic conductor, which exhibits zero reflection phase at one frequency. Resonant frequency at which zero reflection phase occurs, and the bandwidth (reflection phase is within $\pm 90^{\circ}$) depends on the angle of incidence of the incident wave and also on the polarization of the wave (TE or TM). In this work simulation tool CST microwave studio is used for reflection phase computation. The simulation model consists of a unit cell of the structure, enclosed by an air box. To find the variation in the resonant frequency and bandwidth, with the variation in the incident angle, simulation setup shown in Fig. 5 is used. Plane wave is made to incident on the unit cell from the excitation plane, as shown in Fig. 5. Excitation plane (phase extracting plane) is at a distance 0.5λ from the unit cell. Top of the model (excitation plane) is at a distance 0.5λ from the unit cell. To avoid the effect of higher-order harmonics near the structure,

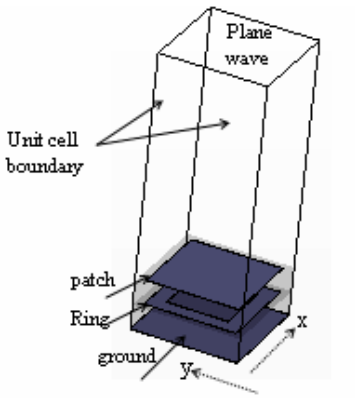

Figure 5. Simulation setup to find reflection phase.

excitation plane must be at a distance greater than or equal to 0.5λ from the top surface of the structure. Unit cell boundaries are used on four side walls. The top is with open boundary, and the bottom is with electric boundary. The phase extracting plane and reflecting surface are at different locations. To restore the reflection phase exactly on the HIS structure, an ideal PEC surface is used as a reference. The scattered fields from a PEC surface are also calculated. The PEC surface is located at the same height as the HIS top surface while phase extracting plane stays the same. The reflected phase from the HIS structure is normalized to the reflected phase from the PEC surface using Equation (1). Therefore, the propagation phase from the distance between the reflecting surface and phase extracting plane canceled out.

$$\text{Reflection Phase} = \theta_{\text{HIS}} - \theta_{\text{PEC}} + \pi \tag{1}$$

In Equation (1), π is added because the PEC surface has a reflection phase of π radians. Reflection phase plots extracted through this model with structural dimensions, $a = 3.5\,\text{mm}$, $w = 3\,\text{mm}$, $g = 0.5\,\text{mm}$, $s = 0.5\,\text{mm}$, $b = 2.5\,\text{mm}$, $h_1 = 0.787\,\text{mm}$, $h_2 = 0.787\,\text{mm}$, $\varepsilon_r = 6.15$, are shown in Fig. 6. The reflection phase of AMCs crosses zero at one frequency. The useful bandwidth of an AMC is in general defined as $+90°$ to $-90°$ on either side of the central frequency.

Figure 6(a) shows the simulation results, when a TE polarized wave is obliquely incident on the unit cell of ring-patch structure at $0°$ to $60°$ insteps of $10°$. As observed from the plot, the resonant frequency and slope of the phase response increase as the incidence

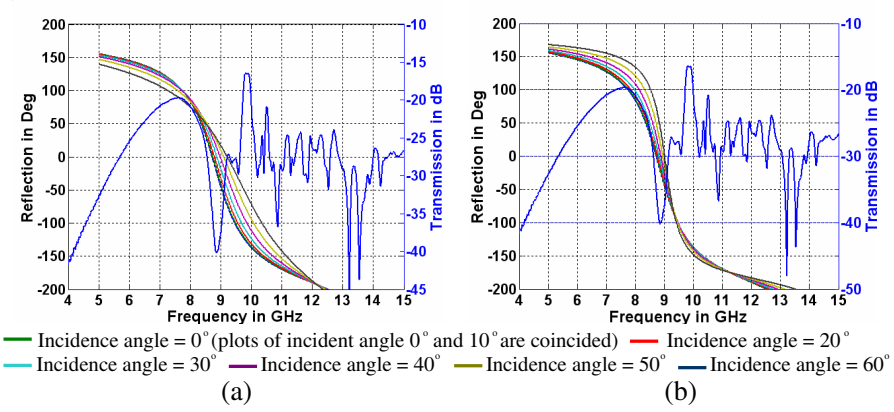

Figure 6. Reflection phase plots. (a) TM polarization, (b) TE polarization.

angle increases. Resonant frequency (frequency at which zero reflection phase occurs) increases from 8.72 GHz to 9.005 GHz as the incident angle is varied from 0° to 60°. ±90° bandwidth decreases from 1.45 GHz to 0.735 GHz as the incident angle is varied from 0° to 60°. The maximum deviation of the resonant frequency is $\Delta f/f_o = 3.27\%$ (f_o — frequency of 0° incidence). TM polarized wave is excited to obliquely incident on the unit cell of ring patch structure at 0° to 60° insteps of 10°, and simulation results are shown in Fig. 6(b). As observed from the plot, the resonant frequency increases and slope of the phase response decreases with the increase in incidence angle. Resonant frequency (frequency at which zero reflection phase occurs) increases from 8.72 GHz to 9.215 GHz as the incident angle is varied from 0° to 60°. ±90° bandwidth increases from 1.45 GHz to 2.63 GHz as the incident angle is varied from 0° to 60°. The maximum deviation of the resonant frequency is 5.68%. In Fig. 6, surface wave suppression and reflection phase plots are combined to show the overlapped surface wave suppression and in-phase reflection bands.

4. MUTUAL COUPLING REDUCTION

There is increased interest in applications of microstrip antennas on high dielectric constant substrates due to their compact size and conformability with the monolithic integrated circuit. However, the utilization of a high dielectric constant substrate has some drawbacks. Among them are a narrower bandwidth and pronounced surface waves. The bandwidth can be recovered using a thick substrate, yet this excites severe surface waves. The generation of surface waves decreases the antenna efficiency and degrades the antenna pattern. Furthermore, it increases the mutual coupling of the antennas in the array. As an application, the proposed structure can be used to reduce the mutual coupling between microstrip antennas.

Simulation setup to demonstrate the mutual coupling is shown in Fig. 7. To demonstrate the reduction in mutual coupling between the microstrip antennas, four columns of the proposed structure are inserted between the antennas as shown in Fig. 7. With the structural parameters $a = 3.5\,\text{mm}$, $w = 3\,\text{mm}$, $g = 0.5\,\text{mm}$, $s = 0.5\,\text{mm}$ $h_1 = h_2 = 0.787\,\text{mm}$, $b = 2.5\,\text{mm}$, the proposed structure has stop band around 9 GHz. With the structural parameters $h_1 = h_2 = 0.787\,\text{mm}$, $w = 4.68\,\text{mm}$, $a = 5.46\,\text{mm}$, $g = 0.78\,\text{mm}$, $s = 0.5\,\text{mm}$, $b = 4.37\,\text{mm}$ the proposed structure has stop band around 7.5 GHz. Microstrip antenna's size is varied to radiate and receive within the stop band of the structure, and the distance between the antennas is 0.75λ at operating frequency. Fig. 8 shows simulated results of the E-plane

coupled microstrip antennas with and without the proposed structure between the antennas. Without the proposed structure, the antennas show a strong mutual coupling. If the proposed structure is employed, the mutual coupling reduces considerably, with maximum suppression of more than 8 dB at resonant frequency as shown in Fig. 8.

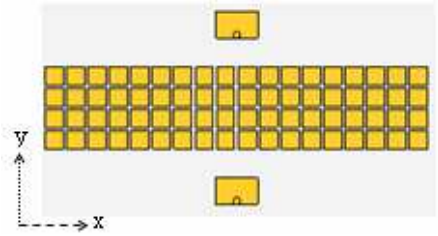

Figure 7. Simulation setup to find E-plane mutual coupling.

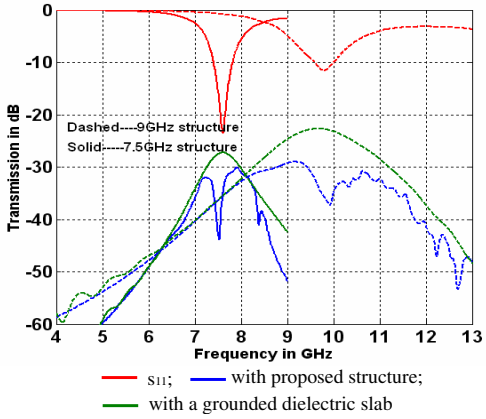

Figure 8. Mutual coupling between microstrip antennas.

5. IMPROVEMENT IN PATTERN PERFORMANCE

To demonstrate the improvement in radiation pattern performance of microstrip antennas over the proposed structure, a rectangular microstrip antenna is designed and simulated to obtain radiation properties. Rectangular microstrip antenna with and without the proposed substrate is shown in Fig. 9. The proposed structure with the structural parameters, $a = 3.5\,\text{mm}$, $w = 3\,\text{mm}$, $g = 0.5\,\text{mm}$,

$s = 0.5\,\text{mm}$ $h_1 = h_2 = 0.787\,\text{mm}$, $b = 2.5\,\text{mm}$, has stop band around 9 GHz. Resonant frequency of the antenna is chosen such that it should be center frequency of surface wave suppression band of the artificial substrate. Rectangular microstrip antenna with artificial substrate under consideration has structural parameters $W = 9.42\,\text{mm}$, $L = 6\,\text{mm}$, substrate material Arlon AD600 $\varepsilon_r = 6.15$, loss tangent $= 0.003$, thickness $h_1 = h_2 = 0.787\,\text{mm}$, and coaxial feed is used. Reference antenna for comparison has dimension $W = 9.42\,\text{mm}$, $L = 6\,\text{mm}$ on ordinary Arlon AD600 substrate of $\varepsilon_r = 6.15$, height $h = 1.58\,\text{mm}$. To keep the antenna dimensions small, the number of unit cells of artificial substrate surrounding the antenna should be limited. The attenuation in the surface wave suppression band will depend on the number of unit cell layers in the structures. This design used four rows of unit cells with an overall dimension of $50\,\text{mm} \times 50\,\text{mm}$. Overall dimension of microstrip antenna over ordinary substrate is also equal to $50\,\text{mm} \times 50\,\text{mm}$.

Usually the E-plane pattern (E-co) of antenna on ordinary substrate is wider than the H-plane pattern (H-co) and has a dip at $\theta = 0$, which is due to high dielectric constant, surface waves and finite size of the ground plane. Radiation patterns of the antenna over the ordinary and proposed substrates, for three different frequencies 9.18 GHz (red), 8.8 GHz (green), 8.56 GHz (blue) within the 10 dB bandwidth are shown in Fig. 10 and Fig. 11 respectively. From simulation results it is observed that with our proposed structure the gain of the antenna is increased, and the radiation pattern of H-plane has been improved significantly. Unlike the E-plane pattern for the reference antenna over the ordinary substrate, the dip at $\theta = 0°$ has disappeared. It indicates the suppression of surface waves with the use of the proposed structure.

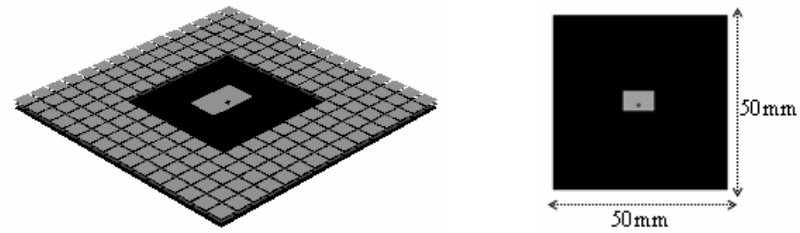

Figure 9. Rectangular microstrip antenna on. (a) Proposed structure, (b) ordinary substrate.

6. EXPERIMENTAL RESULTS

To verify the simulation results experimentally, the proposed structure of dimensions mentioned in Section 3 is printed on a 0.787 mm Arlon AD600 substrate which is backed by a ground plane with array of 16×16 unit cells. Square rings are fabricated on a substrate which

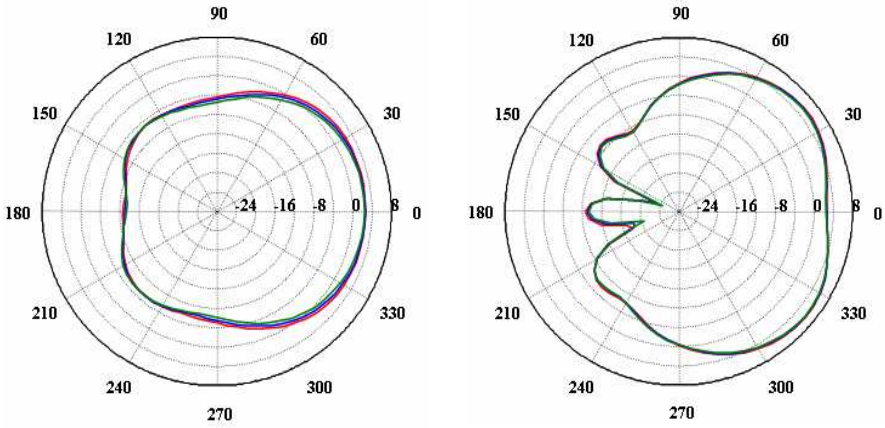

Figure 10. Radiation pattern of antenna on ordinary substrate. (a) H-plane pattern, (b) E-plane pattern.

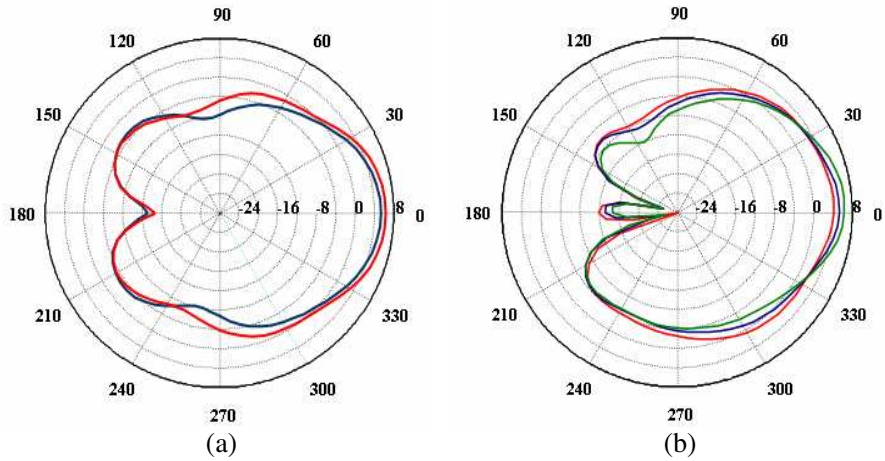

Figure 11. Radiation pattern of antenna on proposed substrate. (a) H-plane pattern, (b) E-plane pattern.

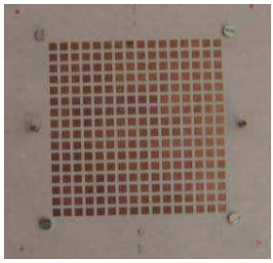

Figure 12. Photograph of the proposed fabricated structure.

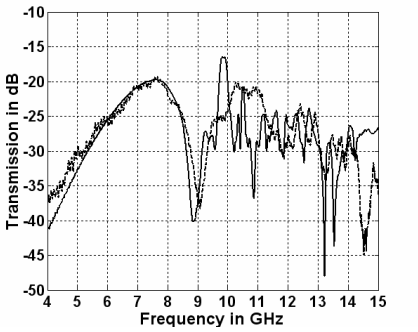

Figure 13. Simulation and measured transmission (S_{21}) between monopoles. - - - - - - Measured; —— simulation.

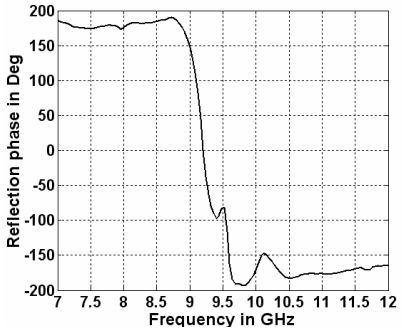

Figure 14. Measured reflection characteristic.

is backed by a metal ground plane. Patches are fabricated on another similar substrate in which the copper metallization is removed from the back side. A photograph of the fabricated structure is shown in Fig. 12 with lower and upper substrate bounded together. Two monopoles of height 8 mm fed with SMA connectors are used for transmission measurement. The transmission (S_{21}) parameter of the structure is measured using Agilent PNA (N5230A). The measured and simulated transmission results using the proposed structure are presented in Fig. 13, where a good agreement can be observed, and the minor differences between the two results can mostly be due to errors occurred during the assembly of the two layers.

Reflection phase measurement is done using waveguide port. A wave guide port is used to incident wave normally on the structure. Reflection phase is extracted from the measured S_{11} parameter using Agilent PNA (N5230A). The measured result is shown in Fig. 14. From the figure it is observed that zero reflection phase frequency is within

the suppression band of the proposed structure. The minor difference in measurement and simulation results may be due to simple wave guide port used for the measurement.

7. DISCUSSION AND CONCLUSIONS

Reflection and surface wave suppression characteristics properties of a stacked ring-patch artificial substrate is studied numerically and experimentally. It has been shown that this structure acts as a high impedance surface within a certain frequency band, providing suppression of surface wave propagation and resulting in a reflection coefficient phase angle of 0°. Simulation studies have proved the reduced mutual coupling between antennas and overall improvement in radiation pattern of the antenna with the proposed structure. Because of the planar nature, this structure can be easily fabricated using planar technologies. From the simulation and experimental studies it is observed that the proposed structure exhibits surface wave suppression similar to the case of mushroom-like structures [1]. The proposed structure can thus be used as a high impedance ground plane for microstrip antennas [1].

REFERENCES

1. Sievenpiper, D. and L. Zhang, "High-Impedance electromagnetic surfaces with a forbidden frequency band," *IEEE Trans. Microw. Theo. Tech.*, Vol. 47, No. 11, 2059–2079, Nov. 1999.
2. Li, L., Q. Chen, and Q. Yuan, "Surface wave suppression band gap and plane wave reflection phase band of mushroomlike photonic band gap structure," *Journal of Applied Physics*, Vol. 103, No. 2, 023513-023513-10, 2008.
3. Luukkonen, O., A. B. Yakovlev, and C. R. Simovski, "Comparative study of surface waves on high-impedance surfaces with and without vias," *Proc. IEEE International Symposium on Antennas and Propagation*, paper s326p3, San Diego, Jul. 5–12, 2008.
4. Yang, F. and A. Aminian, "A novel surface-wave antenna design using a thin periodically loaded ground plane," *Microwave and Optical Technology Letters*, Vol. 47, No. 3, 240–245, Sep. 2005.
5. Simovski, C. R., "High-impedance surfaces having stable resonance with respect to polarization and incidence angle," *IEEE Transactions on Antennas and Propagation*, Vol. 53, No. 3, 908–914, Mar. 2005.

6. McVay, J. and N. Engheta, "High impedance metamaterial surfaces using Hilbert-curve inclusions," *IEEE Microwave and Wireless Components Letters*, Vol. 14, No. 3, 130–132, Mar. 2004.
7. Abedin, M. F., M. Z. Azad, and M. Ali, "Wideband smaller unit-cell planar EBG structures and their application," *IEEE Transactions on Antennas and Propagation*, Vol. 56, No. 3, 903–908, Mar. 2008.
8. Pendry, J. B. and D. R. Smith, "Reversing light: Negative refraction," *Physics Today*, Vol. 57, No. 6, 37–44, 2004.